King Saud University

Arabian Journal of Chemistry

www.ksu.edu.sa
www.sciencedirect.com

ORIGINAL ARTICLE

Effective and highly recyclable ceramic membrane based on amorphous nanosilica for dye removal from the aqueous solutions

CrossMark

Gehan M.K. Tolba [a,b], A.M. Bastaweesy [a], E.A. Ashour [a], Wael Abdelmoez [a], Khalil Abdelrazek Khalil [c,d], Nasser A.M. Barakat [a,b,*]

[a] Chemical Engineering Department, Faculty of Engineering, Minia University, El-Minia, Egypt
[b] BioNanosystem Department, Chonbuk National University, Jeonju 561-756, South Korea
[c] Mechanical Engineering Department, King Saud University, P.O. Box 800, Riyadh 11421, Saudi Arabia
[d] Materials Engineering and Design Department, Aswan University, Aswan, Egypt

Abstract   In this study, an adsorptive ceramic membrane was prepared by a simple dry pressing of a mixture of nanosilica produced from low cost rice husk by hydrothermal technique at sub-critical water conditions, calcium phosphate, and ammonium acetate together and then calcined at 600 °C in air. Optimization of the raw materials ratio was found to be necessary to avoid crack formation during sintering process. The membrane microstructure, dye removal efficiency and the permeation flux of the membranes were investigated. The membrane was tested to remove the methylene blue from aqueous solution. Results show that the removal of the dye increases as the silica content increases in the all given membranes and it decreases with an increase in the ammonium acetate. Moreover, the water flux decreases with an increase in the silica content. The methylene blue adsorbed onto the silica membrane can be removed by calcination and the membrane could be recycled several times without any obvious loss in the adsorption performance. In conclusion, this study demonstrates a convenient strategy to prepare an effective adsorptive membrane, which can be applied as a highly recyclable membrane for the adsorption of organic maters.

* Corresponding author at: BioNanosystem Department, Chonbuk National University, Jeonju 561-756, South Korea. Tel.: +82 632702363; fax: +82 632702348.
  E-mail address: nasser@jbnu.ac.kr (N.A.M. Barakat).
Peer review under responsibility of King Saud University.

ELSEVIER   **Production and hosting by Elsevier**

1. Introduction

Industries pollutants such as organic pollutants and toxic water pollutants are harmful to human health and general well-being of man. For example textile industries produce large volume of colored dye effluents which are toxic and non-biodegradable creating severe environmental problems by releasing toxic and potential carcinogenic substances into the

aqueous phase. The complex structures of the most dyes and their high recalcitrance to degradation are considered a great challenge for decolorization and complete mineralization (Kant et al., 2014; Height et al., 2006). Therefore, various physical, chemical, and biological techniques of alleviating the negative environmental impact of hazardous wastes and toxic water pollutants have been developed. Traditional treatments such as coagulation, flocculation, absorption, and membrane technologies merely concentrate or otherwise transport wastes (Kadirvelu et al., 2003; Zhang et al., 1998; Chatterjee and Mahata, 2002).

Adsorption process is widely used to remove pollutants from wastewaters and can be considered one of the effective methods with high efficiency and no harmful by-products. Moreover, it is generally more attractive from the economic point of view than most other technologies (Barakat et al., 2014a). The major advantages of an adsorption treatment for the control of water pollution are less investment in terms of initial development cost, simple design, easy operations, free from generation of toxic substances, and easy and safe recovery of the adsorbent as well as adsorbate materials (Papić et al., 2004; Keis et al., 2000). Although activated carbon has been extensively used and reviewed as an adsorbent, it still remains expensive for developing countries (Bulut and Aydın, 2006; Altenor et al., 2009). Therefore, other low cost adsorbents have been investigated. The advantage of using agricultural by-products as raw materials for manufacturing activated carbon is that these raw materials are renewable and potentially less expensive to manufacture (Altenor et al., 2009; Ghosh and Bhattacharyya, 2002; Doğan et al., 2004). Rice husk is costless and a widely available agricultural waste which is produced from the processing and refining of rice (Wang et al., 2014). Usually, in many countries, most of the rice husk produced is either burnt producing rice husk ash or dumped as waste (Deiana et al., 2008). About 75–90% of rice husk is organic matters such as cellulose and lignin and the rest (10–25%) are mineral components such as silica, alkalis and trace elements depending on rice variety, soil chemistry, climatic conditions, and even geographic location of growth (Carmona et al., 2013). Rice husk is an excellent and the most efficient source of high-grade amorphous silica (Yalcin and Sevinc, 2001). It is noteworthy mentioning that, according to our best knowledge, exploitation of the amorphous nanosilica in water treatment is very rare in the literature because the introduced amorphous silica nanoparticles have been synthesized using complex and expensive procedures; therefore, they are widely used in the medical fields (Nabeshi et al., 2011; Rahman et al., 2009; Morishita et al., 2012; Yoshida et al., 2013).

The size of adsorbent may play a key role in the adsorption behavior (equilibrium and kinetics) especially if it is nanoscale since the specific surface area becomes larger as its size is reduced (Yang et al., 2006; Barakat et al., 2013a,b,c,2014b,2012; Barakat and Motlak, 2014). Therefore, the content of functional groups responsible for adsorption can be increased by which higher adsorption capacity becomes higher. In addition, the mass transfer rate (especially the external mass transfer) can be increased by a few magnitudes as the size of adsorbent is reduced from macro-meters to nano-meters (Yang and Xing, 2010; Pan et al., 2008). The drawback of the nanoparticles (NPs), however, is the particle separation difficulty after the treatment. Consequently, secondary pollution will be created which might be dangerous than the original

one. If the NPs are embedded in a micro- or ultra-filtration (MF or UF) membrane, it still can act as an adsorbent for the contaminant removal and this will distinctly overcome the need for additional separation step. In addition, membrane processes generally allow a continuous operation and can be combined easily with other separation processes.

Nanotechnology has expanded the range of applications to membrane technologies to improve their performance in wastewater treatment (Kim and Van der Bruggen, 2010). The use of NPs in the manufacturing of membranes allows producing desired structure as well as their function. Researchers have fabricated membranes with metal oxide NPs to increase the novelty of membrane materials, permeability as well as permeate quality. The emergence of new type of ceramic materials and simple fabrication techniques may lead to preparation of low cost membranes (Elma et al., 2013). Ideal adsorptive membranes should have microporous or macroporous structures, available reactive groups for metal ion binding, and chemical and physical stability under harsh conditions (Genç et al., 2003).

The main aim of this study was synthesizing an effective adsorptive membrane based on amorphous nanosilica powder containing the reactive OH^- groups; these effective silica NPs could be extracted from rice husk. The proposed membrane was synthesized from calcium phosphate as a main matrix, ammonium acetate as pores formation agent, and nanosilica as a functional material. It is known that heating of ammonium acetate ($NH_4(CH_3COO)$) in air at high temperature results in complete decomposition and production of some gaseous products (CO_2, NO_x and H_2O). These evolved gases can have a distinct role in creating pores in the introduced membrane. The three constituents were mixed in different ratios and sintered at different temperatures to optimize the performance and mechanical properties of the obtained membrane. Optimization of the raw materials ratio as well as sintering temperature is necessary to avoid crack formation during the sintering process, maintain the amorphous structure of the silica, and maximize the adsorption performance of the produced membrane. The membrane performance was investigated by measuring the removal efficiency of the methylene blue dye.

2. Experimental

2.1. Materials

Rice husk was obtained from a rice mill in Egypt while nitric acid (HNO_3, 60% assay) was obtained from Sigma Aldrich, USA, and distilled water was used to synthesize the nanosilica. Additionally, calcium phosphate ($Ca_3(PO_4)_2$, 98.0 ~103.0%) was obtained from Junsei Chemical Co., Ltd., Japan, while Ammonium Acetate (CH_3COONH_4, 97% assay) was obtained from Chuo-Ku, Tokyo, Japan, which were used for synthesizing the membrane. For the adsorption test, methylene blue dihydrate ($C_{16}H_{18}CIN_3S \cdot 2H_2O$, 95% assay) was obtained from Showa, Japan, and distilled water was used. All chemicals were of analytical grade.

2.2. Preparation of nanosilica

Rice husk was washed several times by distilled water to remove any soluble particles or any other impurities such as

heavy impurities. Then, it was dried in an air oven at about 80 °C for 24 h. After that, the dried rice husk was mixed with nitric acid and distilled water with a ratio of 1:5:5. The solution was well mixed and placed in a teflon crucible inside the reactor. The reactor was made of stainless steel with a height of 15 cm and a diameter of 7 cm. It was placed in the furnace at 160 °C for 2 h. After that, the reactor was immediately cooled down by immersing it directly into a cold-water bath. The product obtained was filtered off, washed several times with distilled water, and dried in vacuum at 60 °C for 24 h for further analysis and applications.

2.3. Fabrication of the adsorptive membrane

Based on our previous studies (Barakat et al., 2008,2009) and others (Sheikh et al., 2011), the extracted hydroxyapatite from the natural bones has better biological characteristics compared to the synthesized one. However, the extraction process should be optimized; subcritical water shows the best performance. Accordingly, from the economic point of view the synthesized one is cheaper. In the introduced application, this ceramic material is used as matrix so we think that there is influence of the biological difference between the two formulations. Therefore, it was decided to use the commercial hydroxyapatite, calcium phosphate. Mixture of calcium phosphate, ammonium acetate, and nanosilica was prepared by adding different amounts of ammonium acetate (20%, 30%, 40%, and 50%) and different amounts of nanosilica (5%, 10%, 15%, and 20%) with 800 mg of calcium phosphate. The mixture was well mixed and placed into the mold. After that, the mixed powders were subjected to a high pressure force for consolidation into a single mass to form the membrane disk. The formed membrane was initially dried for 24 h at 80 °C and then calcined in the air at 600 °C for 120 min, with a heating rate of 2 °C/min. The prepared membranes have been labeled as shown in Table 1. It is noteworthy mentioning that increasing of ammonium acetate more than 50 wt% led to produce fragile membrane.

2.4. Characterization of the nanosilica

Information on the phase and crystallinity was obtained by using Rigaku X-ray diffractometer (XRD, Rigaku, Japan) with Cu Kα ($\lambda = 1.540$ Å) radiation over Bragg angle ranging from 10° to 80°. Surface morphology was studied by field-emission scanning electron microscope equipped with EDX analysis tool (FESEM, Hitachi S-7400, Japan). Moreover, High resolution images were obtained with transmission electron microscope (TEM, JEOL JEM-2010, Japan) operated at 200 kV equipped with EDX analysis.

2.5. Characterization of the membrane

Surface morphology of the membranes was investigated by scanning electron microscope (SEM, JEOL JSM-5900, Japan). The surface and cross-section of the membranes were studied by field-emission scanning electron microscope equipped with EDX analysis tool (FESEM, Hitachi S-7400, Japan). The existence of NP in the membranes was detected by Energy Dispersive X-ray (EDX) Spectroscopy.

2.6. Batch adsorption experiments

The adsorption of MB in aqueous solution on the as-prepared nanosilica was in a batch experiment by adding 50 mg of the nanosilica into 50 ml of a different initial concentration (10, 30, and 50 ppm) of MB aqueous solution. With stirring at room temperature, samples were taken out at regular time intervals. After that, the supernatant solution was separated from adsorbent by centrifugation at 5000 rpm for 15 min. Then, the concentration of MB was determined by a spectrophotometer.

After the determination of the sorbent adsorption capacity, the adsorption efficiency of the membranes was examined by passing a 12 ml of 10 ppm methylene blue solution through the membrane. Then the permeated dye solution was recycled to pass through the membrane again; this process was repeated for five successive cycles. Samples were taken after each cycle and the time was recorded to calculate the flux.

The amount of MB adsorbed per unit mass of the adsorbent was evaluated by using the mass balance equation (Eq. (1)) and the percentage of the MB removal was evaluated as well (Eq. (2)).

$$q = \frac{(C_0 - C)V}{W} \tag{1}$$

$$Removal \% = \frac{C_o - C}{C_o} \times 100 \tag{2}$$

where q is the solid phase MB concentration (mg/g), C_0 is the initial MB concentration in the liquid phase (ppm), C is the liquid phase concentration (ppm), V is the volume of dye solution (l), and m is the mass of adsorbent used (g). Finally, the adsorption capacity and the percentage of the dye removal were plotted. The exhausted membranes were regenerated by calcination in air at 450 °C for 90 min, and then reused for the adsorption again. The supernatant solutions were analyzed by UV–vis spectroscopy. In addition, absorbance of the solution was determined using an UV–via spectrophotometer at 664 nm (λ_{max}) corresponding to the maximum absorption of MB.

3. Results and discussion

3.1. Characterization of the nanosilica

To extract the amorphous silica nanoparticles from rice husk the following procedure was utilized. First, the rice husk was washed with distilled water to remove any impurities that can contaminate the final silica product as well as washing can dissolute some soluble substances, including metal salts, allowing a preliminary chemical purification. Second, the

Table 1 Matrix of membrane compositions.

NH$_3$COONH$_4$ (%)	SiO$_2$ (%)			
	5	10	15	20
10	AA10-S5	AA10-S10	AA10-S15	AA10-S20
20	AA20-S5	AA20-S10	AA20-S15	AA20-S20
30	AA30-S5	AA30-S10	AA30-S15	AA30-S20
40	AA40-S5	AA40-S10	AA40-S15	AA40-S20
50	AA50-S5	AA50-S10	AA50-S15	AA50-S20

hydrothermal process at sub-critical water conditions was carried out at high-temperature, high-pressure, and acidic media with strong oxidation activities (using nitric acid). At those conditions the organic compounds can be decomposed, and the trace metals can be turned into soluble ions; then, silica can be obtained. The morphology of SiO_2-based NPs is illustrated in Fig. 1A. As shown in the figure, the diameter of each NP ranges from 10 to 30 nm indicating that the NP is nanosized. The as-prepared powder consists of spherical particles with a poor agglomeration and aggregation that takes place during the hydrothermal process. The NPs seem to form irregular clusters which may make the overall sizes larger. As a result, the NPs may become easier to stay in the membrane instead of flowing through it during the adsorption operation. Furthermore, TEM micrographs provide more accurate information on the particle size and surface morphology of the produced nanosilica. As displayed in Fig. 1B, the absence of the atomic planes on the image indicates amorphous structure of the obtained nanosilica.

The crystallization phase of the silica powder was displayed by XRD spectrum. As displayed in Fig. 2A, a wide and a broad peak between 17° and 38° centered at 22° corresponds to the crystal planes of (1 0 1) indicating the amorphous (cristobalite) nature of the silica (JCPDS card No 21-1272) (Lv et al., 2013). In addition, the nonappearance of other sharp peaks of possible impurities such as alkaline earth metals confirms the

purity of the as-derived silica. Furthermore, the chemical composition of silica was confirmed by EDX. The analysis as shown in Fig. 2B identifies the presence of silicon(Si) and oxygen(O) at a calculated 1:2 atomic ratio, and the absence of other elements reported in rice husk such as Ca, K, Na, Mg, Fe, Al, and Mg (Gu et al., 2013). The presence of low amount of carbon could be from the measurements.

3.2. Characterization of the prepared membranes

Surface SEM images of the membranes fired at 600 °C for 2 h with a heating rate of 2 °C/min are illustrated in Fig. 3. As shown, there is a rough surface morphological structure, and an irregular pore size and pore shape as well for all membranes. As presented in Fig. 3 A, for the specimen made of 10% AA, there are only spot contacts among solid particles or very small pore size. However, with the addition of ammonium acetate as commonly practiced as a pore forming agent, no crack formation is found. The pore size increased with increasing the amount of the ammonium acetate while the shape of the pores became slightly uniform. Additionally, it was observed that increasing the mass ratio of ammonium acetate more than 50% in the membrane could not form stable membrane; the obtained membrane is fragile.

Fig. 4A shows the FE-SEM for the membrane (AA40-S10). As shown in the figure, there are many uniform pores
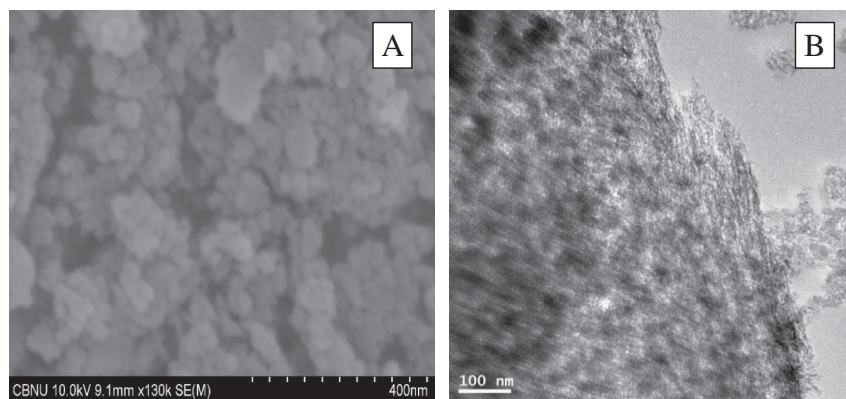

Figure 1   (A) FE-SEM images of the obtained nanosilica and (B) TEM images for the obtained nanosilica.
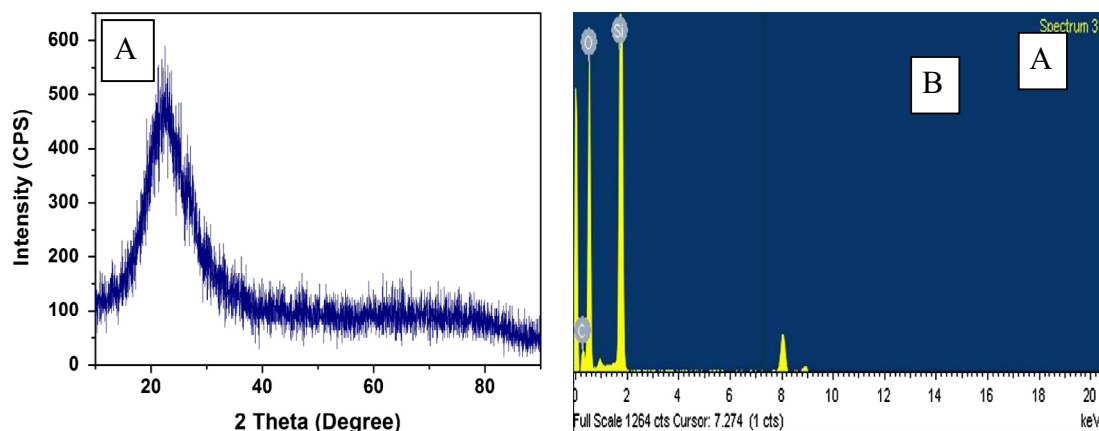

Figure 2   (A) XRD pattern of the obtained nanosilica and (B) EDX spectrometric data of silica produced from RHA.
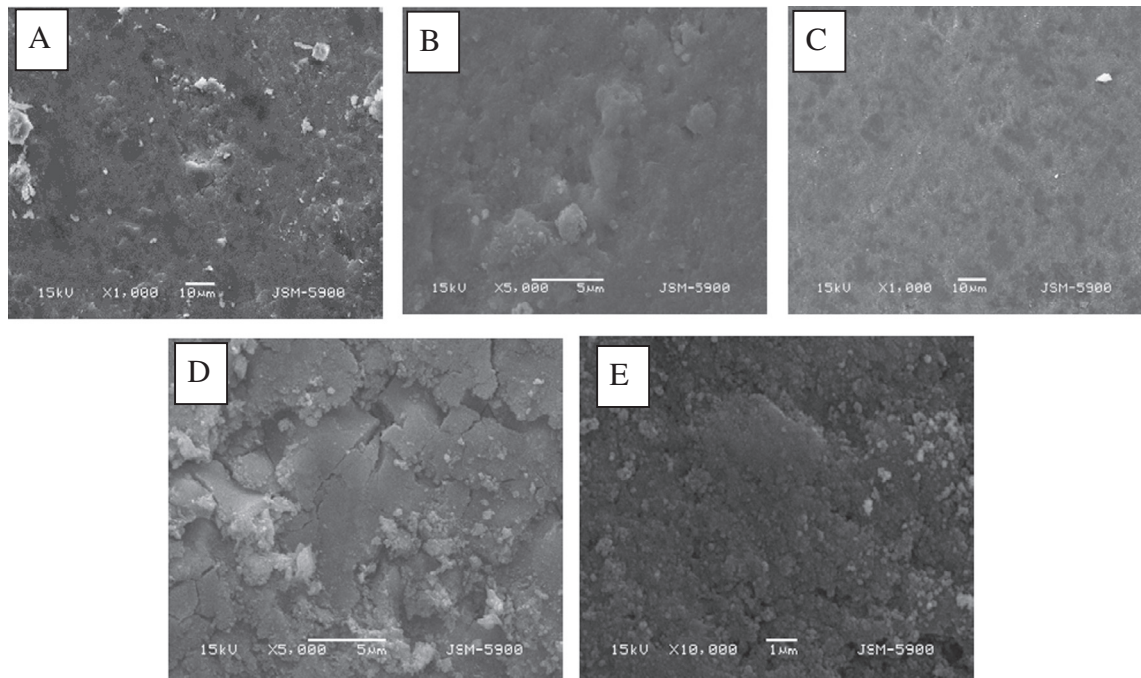
Figure 3 SEM images for (A) AA10-S20, (B) AA20-S20, (C) AA30-S20, (D) AA40-S20, and (E)AA50-S20.
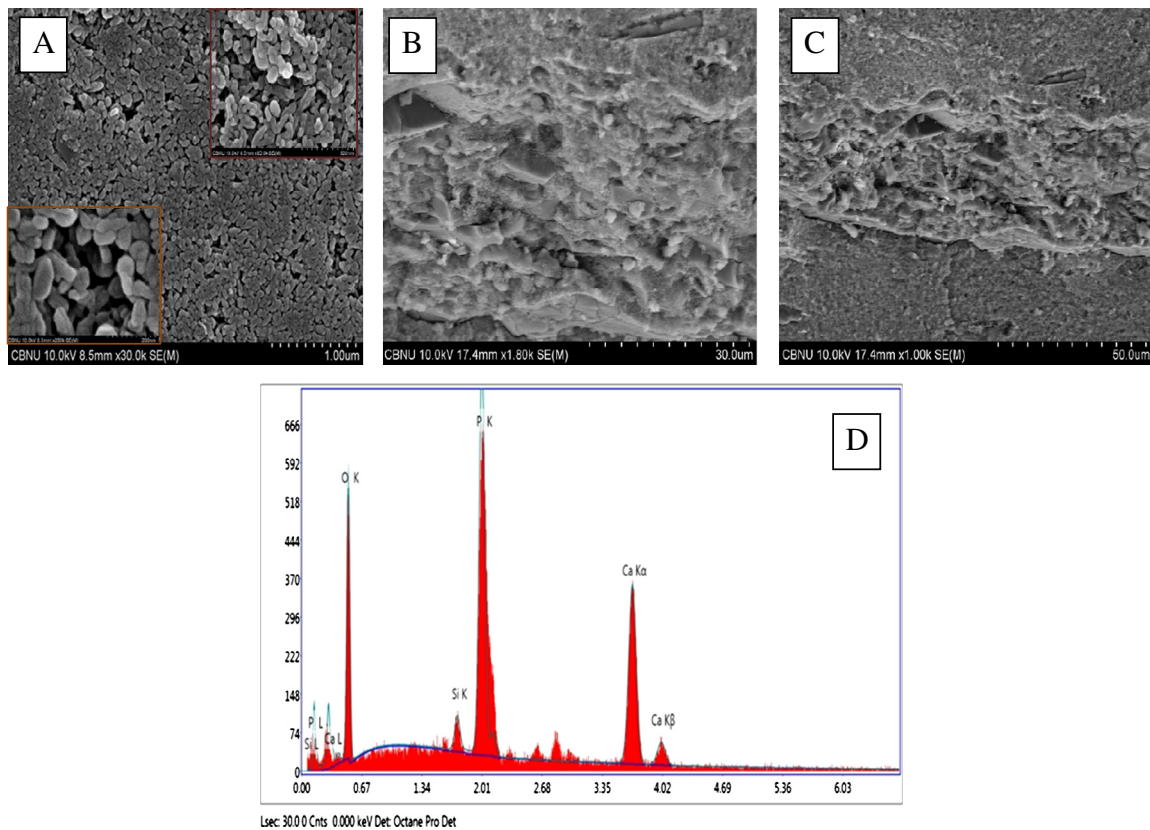

Figure 4 (A) FESEM images, (B and C) cross-section FESEM micrograph, (D) EDX of AA40-S10.

distributed all over the membrane surface. As the magnification increases, the pores became clear and almost have a special shape in the upper and lower inset. In addition, the cross-section FE-SEM micrograph in Fig. 4(B) of the prepared silica membrane shows that there are no cracks. The connection between interior layers and top-layer is also good.

Moreover, it can be seen from the figure that there is a uniform distribution for the silica nanoparticles through the whole membrane (Red circles) while the silica nanoparticles are uniformly distributed all over the membrane. Furthermore, the pore size distribution of the top-layer becomes narrower than that of the inter layer despite the effect of layer thickness. There was a quick membrane formation rate and there were the coarser pores in the interlayer membrane [19]. Moreover, more macrovoids are formed as the silica NPs content increases. This is credited to the hydrophilic property of the SiO_2 NPs which draws more water during the phase inversion
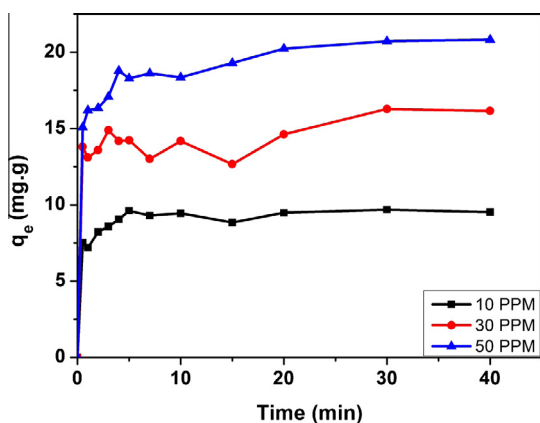

Figure 5   The adsorptive capacity of the obtained nanosilica.

process. The EDX analysis (Fig. 4D) of the membrane can further confirm the presence of the SiO_2 NPs in the membrane.

3.3. Adsorption performance of the nanosilica

Fig. 5 shows the effects of contact time on the adsorption capacity of MB onto nanosilica at different initial concentrations (10, 30, and 50 ppm). It is observed that the adsorption capacity of MB onto the adsorbent considerably increases during the initial stage, more than 80% of the MB within 5 min at the initial MB concentration of 10 ppm, and then at a slow speed. The increasing trend not stops until a state of equilibrium is acquired after 30 min. This could be assigned to the fact that most vacant surface sites are available for adsorption during the initial stage and the remaining vacant surface sites are hard to be utilized due to repulsive forces between the MB molecules on SiO_2 and the bulk phase as well as to the high surface area of the produced nanosilica. Moreover, the absence of the impurities has a substantial effect on the quality and purity of the silica produced from rice husk. The adsorption of MB onto silica depends largely on the initial MB concentrations since initial MB concentrations can provide a driving force to overcome the mass transfer resistance of the dye.

The regeneration experiments were conducted in the 50 mL of 10, 30, and 50 ppm MB solutions with 20 mg SiO_2 sample at room temperature for 30 min. The MB-adsorbed SiO_2 is collected through natural settlement for 10 min, calcined in air at 450 °C for 90 min, and then reused for the adsorption again.
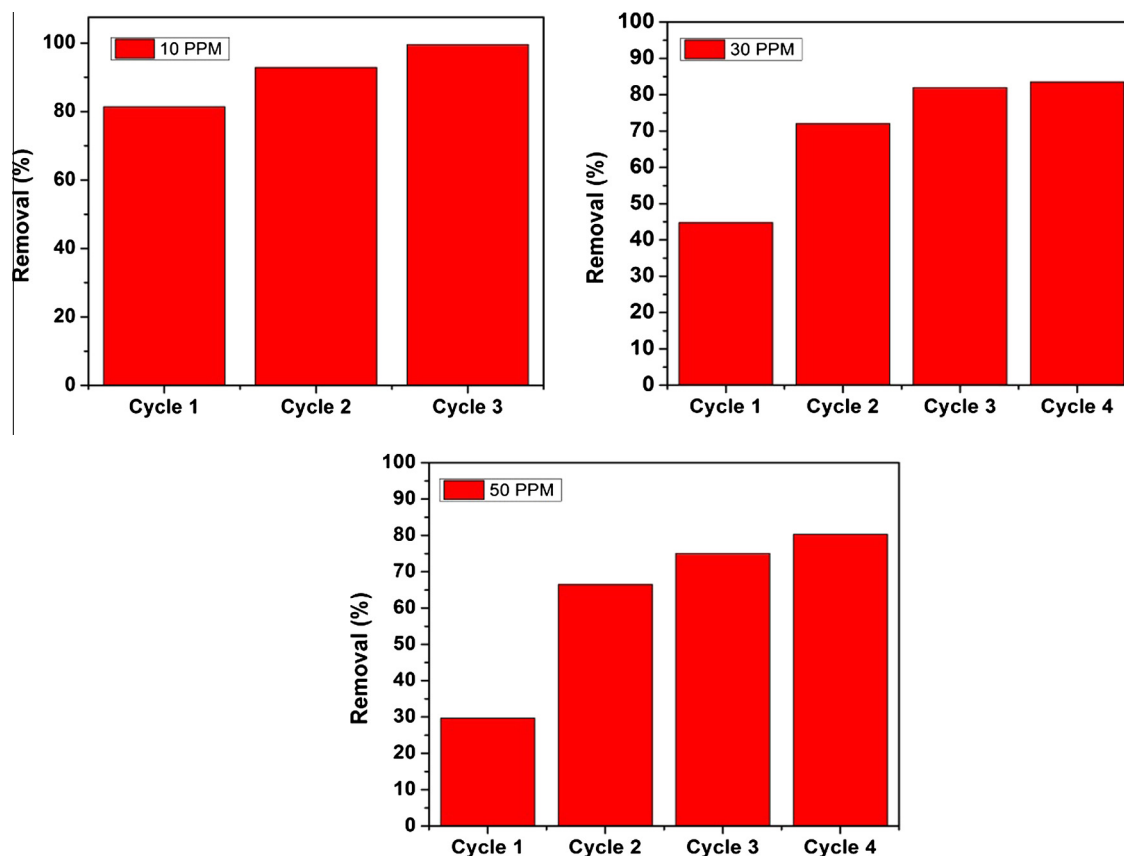

Figure 6   Removal efficiency of MB onto SiO_2 in four successive cycles at different dye concentrations: 10, 30 and 50 ppm.

The percentage of MB removal for each cycle at different initial concentrations 10, 30, and 50 PPM after 30 min is calculated according to Eq. (2) (Kannan and Sundaram, 2001) and presented in Fig. 6. About 99.6% of MB were removed in 30 min in the third cycle for the initial concentration 10 PPM as well as increased for the other initial concentrations. The complete removal observed can be related to the strong interactions between the MB molecules and the adsorbent surface as well as to its high surface area.

It is known that in a batch type adsorption systems, the rate of removal of adsorbate species from aqueous solution is controlled primarily by the rate of transport of the adsorbate species from the outer sites to the interior sites of the adsorbent particles (Kannan and Sundaram, 2001). The increase in the

Figure 7 Schematic of membrane adsorption test.

adsorptive efficiency after each cycle confirms the reusability of nanosilica for the removal of MB with a very high efficiency. Notably, the calcination process enhanced the adsorption capacity for the nanosilica. The presence of the silanol groups on the silica surface gives the amorphous silica its chemical activity. Thus, adsorption on the silica surface requires that the surface is dried. After adsorption and calcination processes, silanol groups become extremely reactive which enhances the performance (Krysztafkiewicz et al., 2002).

3.4. Adsorption performance of the membranes

The adsorptive activity of the prepared membranes was evaluated by adsorption of methylene blue from the aqueous solution. The schematic diagram used to investigate the adsorption performance of the membranes and the flux through the membrane is illustrated in Fig. 7. Typically, 12 mL of a 10 ppm MB aqueous solution was passed through the membrane. Then passing dye solution was through the membrane again and repeated for five cycles. After each cycle, samples were taken and the time was recorded to calculate the permeate flux. Two experiments for each membrane were done and the average was used. As shown in Fig. 8 and Fig. 9, the results suggested that the removal efficiency for all membranes increases with an increase in the amount of silica content in the membranes. Such membranes usually contain active OH^- functional groups on their pore surface and bind dye ions by adsorption where dye ions are removed from the aqueous
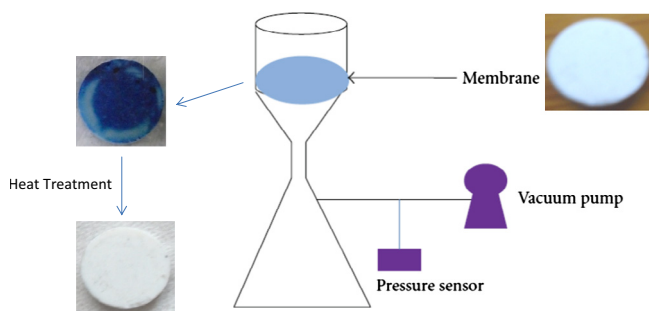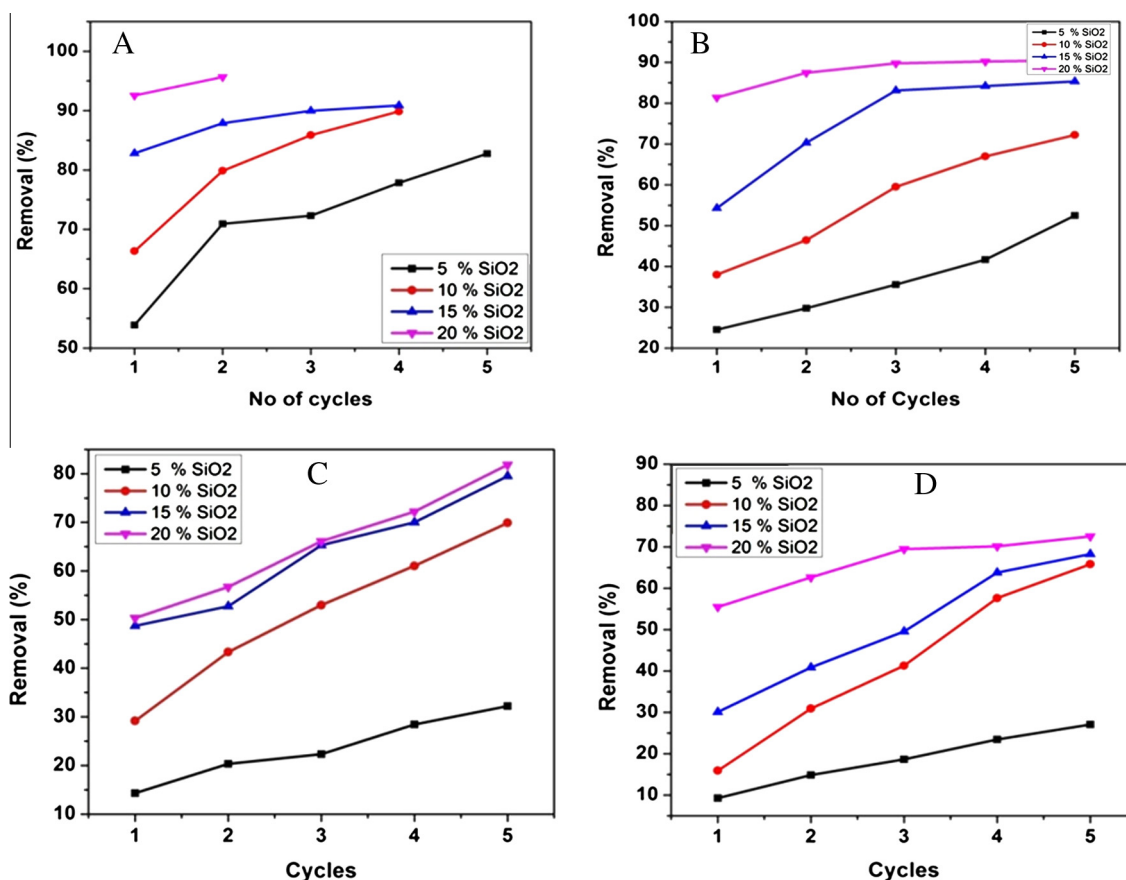

Figure 8 Removal efficiency of the membrane (A) 20% AA, (B) 30% AA, (C) 40% AA, and (D) 50% AA.

solutions during contact with the surface and the interior pores of the membrane, even if the pore size of the membrane is much larger than the size of dye molecules. That may be due to the increase of the adsorptive active sites. It is interesting to note that almost all the dye removed by membrane AA20S20 is credited to the presence of many small pores which contain large amount of silica nanoparticles. Moreover, the removal efficiency decreases as the ammonium acetate increases due to increasing of the pore size (see Fig. 9)

Dried membrane samples were subjected to the feed of MB concentration and were fixed at 12 ml of 10 ppm at room temperature. As shown in Fig. 10, it is obvious that the permeate flux decreased sharply with an increase in the silica content from 40 m^3/m^2 d for AA20-S5 to 7 m^3/m^2 d for AA20-S20. The results were attributed to the following three reasons: (1) the presence of reactive precipitates of MB, which assembled and aggregated to form a cake on the membrane surface and in the membrane pores; (2) fouling of the membrane by adsorption of MB; and (3) a deposited layer near the membrane surface for the concentration polarization effect. The MB adsorbent layer on the surface and on the pores offered more resistance against water flux through the membrane. Another important finding which can be observed in Fig. 10
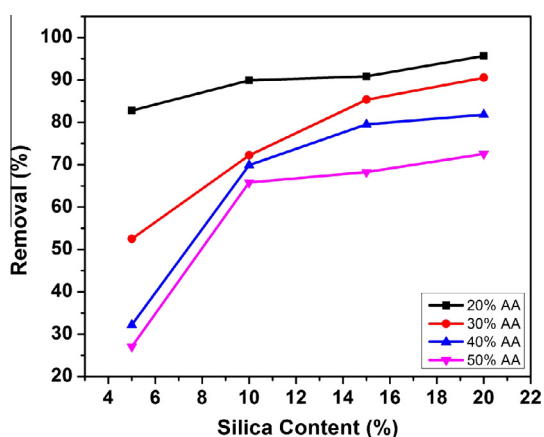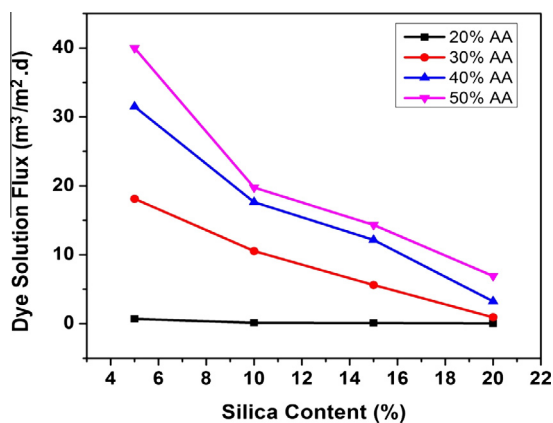
is that increasing the silica content leads to decrease the daily flux for all formulations which can be attributed to closing of the pores.

3.5. Filtration tests

Filtration means using silica-free membrane, so it is expected that the dye removal is achieved due to filtration in the absence of adsorbent. Consequently, dye removing in case of silica-containing membranes could be assigned to the silica adsorption capacity. This test is very important to show the influence of silica incorporation. Filtration experiments were performed for silica-free membranes (20, 30, 40, and 50% AA) to confirm that the removal of the dye molecules occurred due the adsorption only with feed about 12 ml of 10 ppm of MB and the active surface of each membrane was approximately 0.64 cm^2 as shown in Fig. 11. In general, the removal efficiency decreased with an increase in the amount of ammonium acetate; the removal percentage of the MB decreased from 16 for the membrane containing 20% ammonium acetate to 5 for the membrane containing 50% ammonium acetate. On the other hand, when using nanosilica-based membranes, the removal of the methylene blue reaches to more than 80% for the initial concentration of 10 ppm for the membrane containing 20% AA and 10% SiO_2 compared to only 16% removal for the membranes AA20% without silica. The results infer that the adsorption process is better than the filtration process for the removal of MB. Generally, it is believed that removal efficiency can be enhanced by adsorption of adsorbate through the membrane.

3.6. Recyclability

Regeneration ability as well as stability of the adsorptive membrane during the adsorption process is essential to its practical application. Interestingly, the membrane could be renewed by calcination. The insets (from left to right) in Fig. 12 show the images of the obtained nanosilica before and after the adsorption process of MB and then after calcination. As shown in the figure, all MB molecules were removed after the calcination process. The calcination of the adsorbent could retain the high removal efficiency during the six successive cycles as shown in
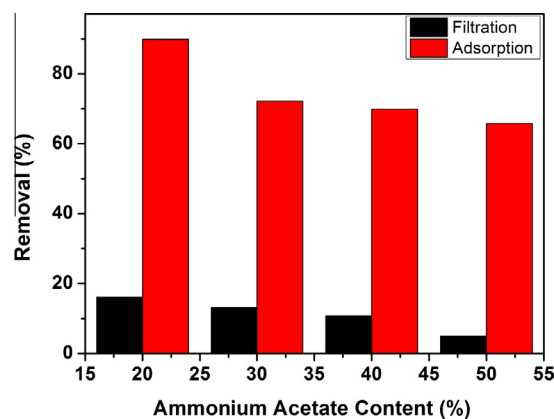

Figure 9 Effect of the Silica content on the removal efficiency of the MB.

Figure 10 Effect of the silica content on the daily dye flow rate (m^3/m^2).

Figure 11 Removal efficiency due to the adsorption and filtration processes.
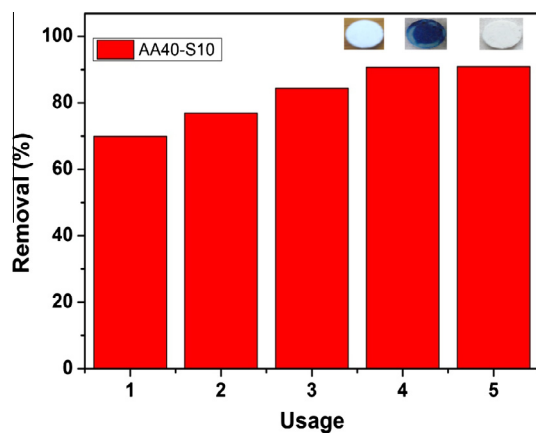
Figure 12 Efficiency of the prepared membrane for several usages for MB removal (AA40-S10).

the figure. Therefore, a membrane with an excellent adsorption performance and regeneration property can be extended to environmental application for wastewater treatment. Thus, reactions on the silica membrane require that the surface is dried in a vacuum in order to remove water. After this procedure, silanol groups become more active (Parida et al., 2006). It is noteworthy mentioning that the influences of other process parameters such as temperature and pH on the adsorption efficiency of the utilized functional nanoparticles have been intensively studied in our previous report (Tolba et al., 2015).

4. Conclusion

The obtained results from this study can be exploited to draw the following conclusions:

1. Amorphous silica nanoparticles can be extracted from the rice husk using the subcritical water with nitric acid as an oxidizing agent for the organic and inorganic ingredients.
2. Low cost porous mineral based ceramic membranes containing the as-obtained amorphous nanosilica as a strong adsorbing material and calcium phosphate can be developed by dry pressing method followed by calcination in air.
3. Addition of ammonium acetate up to 50 wt% can enhance the porosity of the final membrane. However, fragile membranes will be produced if the ammonium content increases than the aforementioned threshold.
4. Increasing the silica nanoparticles content distinctly enhances the adsorption capacity of the introduced membranes at all the investigated ammonium acetate contents; however, considerable negative influence on the daily flux has been observed; 5 wt% silica can be considered the optimum composition.
5. Due to formation of active silanol group on the surface of the functional nanoparticles with successive utilization of the introduced membrane, good recyclability was observed.
6. Overall, the results suggest that the produced silica membrane could be explored as a new adsorbent with high efficiency and recyclability for removing organic dye pollutants from aqueous solution. These low cost mineral-based membranes may be the potentially excellent candidates for the use in wastewater treatment.

References

Altenor, S., Carene, B., Emmanuel, E., Lambert, J., Ehrhardt, J.-J., Gaspard, S., 2009. Adsorption studies of methylene blue and phenol onto vetiver roots activated carbon prepared by chemical activation. J. Hazard. Mater. 165 (1), 1029–1039.

Barakat, N.A., Motlak, M., 2014. Co x Ni y-decorated graphene as novel, stable and super effective non-precious electro-catalyst for methanol oxidation. Appl. Catal., B 154, 221–231.

Barakat, N.A., Khalil, K., Sheikh, F.A., Omran, A., Gaihre, B., Khil, S.M., Kim, H.Y., 2008. Physiochemical characterizations of hydroxyapatite extracted from bovine bones by three different methods: extraction of biologically desirable HAp. Mate. Sci. Eng.: C 28 (8), 1381–1387.

Barakat, N.A., Khil, M.S., Omran, A., Sheikh, F.A., Kim, H.Y., 2009. Extraction of pure natural hydroxyapatite from the bovine bones bio waste by three different methods. J. Mater. Process Technol. 209 (7), 3408–3415.

Barakat, N.A., Khalil, K.A., Kim, H.Y., 2012. Toward facile synthesizing of diamond nanostructures via nanotechnological approach: Lonsdaleite carbon nanofibers by electrospinning. Mater. Res. Bull. 47 (9), 2140–2147.

Barakat, N.A., Abdelkareem, M.A., El-Newehy, M., Kim, H.Y., 2013a. Influence of the nanofibrous morphology on the catalytic activity of NiO nanostructures: an effective impact toward methanol electrooxidation. Nanoscale Res. Lett. 8 (1), 1–6.

Barakat, N.A., Abdelkareem, M.A., Kim, H.Y., 2013b. Ethanol electro-oxidation using cadmium-doped cobalt/carbon nanoparticles as novel non precious electrocatalyst. Appl. Catal, A 455, 193–198.

Barakat, N.A., El-Deen, A.G., Shin, G., Park, M., Kim, H.Y., 2013c. Novel Cd-doped Co/C nanoparticles for electrochemical supercapacitors. Mater. Lett. 99, 168–171.

Barakat, N., Nassar, M., Farrag, T., Mahmoud, M., 2014a. Effective photodegradation of methomyl pesticide in concentrated solutions by novel enhancement of the photocatalytic activity of TiO2 using CdSO4 nanoparticles. Environ. Sci. Pollut. Res. 21 (2), 1425–1435.

Barakat, N.A., El-Newehy, M., Al-Deyab, S.S., Kim, H.Y., 2014b. Cobalt/copper-decorated carbon nanofibers as novel non-precious electrocatalyst for methanol electrooxidation. Nanoscale Res. Lett. 9 (1), 2.

Bulut, Y., Aydın, H., 2006. A kinetics and thermodynamics study of methylene blue adsorption on wheat shells. Desalination 194 (1), 259–267.

Carmona, V., Oliveira, R., Silva, W., Mattoso, L., Marconcini, J., 2013. Nanosilica from rice husk: extraction and characterization. Ind. Crops Prod. 43, 291–296.

Chatterjee, D., Mahata, A., 2002. Visible light induced photodegradation of organic pollutants on dye adsorbed TiO$_2$ surface. J. Photochem. Photobiol. A: Chem. 153 (1), 199–204.

Deiana, C., Granados, D., Venturini, R., Amaya, A., Sergio, M., Tancredi, N., 2008. Activated carbons obtained from rice husk: influence of leaching on textural parameters. Indust. Eng. Chem. Res. 47 (14), 4754–4757.

Doğan, M., Alkan, M., Türkyilmaz, A., Özdemir, Y., 2004. Kinetics and mechanism of removal of methylene blue by adsorption onto perlite. J. Hazard. Mater. 109 (1), 141–148.

Elma, M., Yacou, C., Diniz da Costa, J.C., Wang, D.K., 2013. Performance and long term stability of mesoporous silica membranes for desalination. Membranes 3 (3), 136–150.

Genç, Ö., Soysal, L., Bayramoğlu, G., Arıca, M., Bektaş, S., 2003. Procion green H-4G immobilized poly (hydroxyethylmethacrylate/chitosan) composite membranes for heavy metal removal. J. Hazard. Mater. 97 (1), 111–125.

Ghosh, D., Bhattacharyya, K.G., 2002. Adsorption of methylene blue on kaolinite. Appl. Clay Sci. 20 (6), 295–300.

Gu, S., Zhou, J., Luo, Z., Wang, Q., Ni, M., 2013. A detailed study of the effects of pyrolysis temperature and feedstock particle size on the preparation of nanosilica from rice husk. Indust. Crops Prod. 50, 540–549.

Height, M.J., Pratsinis, S.E., Mekasuwandumrong, O., Praserthdam, P., 2006. Ag–ZnO catalysts for UV-photodegradation of methylene blue. Appl. Catal. B: Environ. 63 (3), 305–312.

Kadirvelu, K., Kavipriya, M., Karthika, C., Radhika, M., Vennilamani, N., Pattabhi, S., 2003. Utilization of various agricultural wastes for activated carbon preparation and application for the removal of dyes and metal ions from aqueous solutions. Bioresour. Technol. 87 (1), 129–132.

Kannan, N., Sundaram, M.M., 2001. Kinetics and mechanism of removal of methylene blue by adsorption on various carbons—a comparative study. Dyes Pigments 51 (1), 25–40.

Kant, S., Pathania, D., Singh, P., Dhiman, P., Kumar, A., 2014. Removal of malachite green and methylene blue by $Fe_{0.01}Ni_{0.01}Zn_{0.98}O$/polyacrylamide nanocomposite using coupled adsorption and photocatalysis. Appl. Catal. B: Environ. 147, 340–352.

Keis, K., Lindgren, J., Lindquist, S.-E., Hagfeldt, A., 2000. Studies of the adsorption process of Ru complexes in nanoporous ZnO electrodes. Langmuir 16 (10), 4688–4694.

Kim, J., Van der Bruggen, B., 2010. The use of nanoparticles in polymeric and ceramic membrane structures: review of manufacturing procedures and performance improvement for water treatment. Environ. Pollut. 158 (7), 2335–2349.

Krysztafkiewicz, A., Binkowski, S., Jesionowski, T., 2002. Adsorption of dyes on a silica surface. Appl. Surf. Sci. 199 (1), 31–39.

Lv, P., Zhao, H., Wang, J., Liu, X., Zhang, T., Xia, Q., 2013. Facile preparation and electrochemical properties of amorphous SiO_2/C composite as anode material for lithium ion batteries. J. Power Sources 237, 291–294, doi: http://dx.doi.org/10.1016/j.jpowsour.2013.03.054.

Morishita, Y., Yoshioka, Y., Satoh, H., Nojiri, N., Nagano, K., Abe, Y., Kamada, H., S-i, Tsunoda., Nabeshi, H., Yoshikawa, T., 2012. Distribution and histologic effects of intravenously administered amorphous nanosilica particles in the testes of mice. Biochem. Biophys. Res. Commun. 420 (2), 297–301.

Nabeshi, H., Yoshikawa, T., Matsuyama, K., Nakazato, Y., Matsuo, K., Arimori, A., Isobe, M., Tochigi, S., Kondoh, S., Hirai, T., 2011. Systemic distribution, nuclear entry and cytotoxicity of amorphous nanosilica following topical application. Biomaterials 32 (11), 2713–2724.

Pan, B., Lin, D., Mashayekhi, H., Xing, B., 2008. Adsorption and hysteresis of bisphenol A and 17α-ethinyl estradiol on carbon nanomaterials. Environ. Sci. Technol. 42 (15), 5480–5485.

Papić, S., Koprivanac, N., Lončarić Božić, A., Meteš, A., 2004. Removal of some reactive dyes from synthetic wastewater by combined Al (III) coagulation/carbon adsorption process. Dyes Pigments 62 (3), 291–298.

Parida, S.K., Dash, S., Patel, S., Mishra, B., 2006. Adsorption of organic molecules on silica surface. Adv. Colloid Interf. Sci. 121 (1), 77–110.

Rahman, A., Seth, D., Mukhopadhyaya, S.K., Brahmachary, R.L., Ulrichs, C., Goswami, A., 2009. Surface functionalized amorphous nanosilica and microsilica with nanopores as promising tools in biomedicine. Naturwissenschaften 96 (1), 31–38.

Sheikh, F.A., Kanjwal, M.A., Macossay, J., Muhammad, M.A., Cantu, T., Barakat, N.A., Kim, H.Y., 2011. Fabrication of mineralized collagen from bovine waste materials by hydrothermal method as promised biomaterials. J. Biomater. Tissue Eng. 1 (2).

Tolba, G.M., Barakat, N.A., Bastaweesy, A., Ashour, E., Abdelmoez, W., El-Newehy, M.H., Al-Deyab, S.S., Kim, H.Y., 2015. Effective and highly recyclable nanosilica produced from the rice husk for effective removal of organic dyes. J. Ind. Eng. Chem.

Wang, G., Wang, D., Kuang, S., Xing, W., Zhuo, S., 2014. Hierarchical porous carbon derived from rice husk as a low-cost counter electrode of dye-sensitized solar cells. Renew. Energy 63, 708–714.

Yalcin, N., Sevinc, V., 2001. Studies on silica obtained from rice husk. Ceram. Int. 27 (2), 219–224.

Yang, K., Xing, B., 2010. Adsorption of organic compounds by carbon nanomaterials in aqueous phase: polanyi theory and its application. Chem. Rev. 110 (10), 5989–6008.

Yang, K., Zhu, L., Xing, B., 2006. Adsorption of polycyclic aromatic hydrocarbons by carbon nanomaterials. Environ. Sci. Technol. 40 (6), 1855–1861.

Yoshida, T., Yoshioka, Y., Tochigi, S., Hirai, T., Uji, M., K-i, Ichihashi., Nagano, K., Abe, Y., Kamada, H., S-i, Tsunoda., 2013. Intranasal exposure to amorphous nanosilica particles could activate intrinsic coagulation cascade and platelets in mice. Part Fibre Toxicol. 10 (41), 8977-8910.

Zhang, F., Zhao, J., Shen, T., Hidaka, H., Pelizzetti, E., Serpone, N., 1998. TiO2-assisted photodegradation of dye pollutants II. Adsorption and degradation kinetics of eosin in TiO_2 dispersions under visible light irradiation. Appl. Catal. B: Environ. 15 (1), 147–156.